

MC^3 : Memory Contention based Covert Channel Communication on Shared DRAM System-on-Chips

Ismet Dagli

Computer Science Department
Colorado School of Mines
Golden, CO, USA
ismetdagli@mines.edu

James Crea

Computer Science Department
Colorado School of Mines
Golden, USA
jcrea@mines.edu

Soner Seckiner

Department of Electrical and Computer Engineering
University of Rochester
Rochester, NY, USA
sseckine@ur.rochester.edu

Yuanchao Xu

Computer Science Department
University of California Santa Cruz
Santa Cruz, CA, USA
yxu314@ucsc.edu

Selçuk Köse

Department of Electrical and Computer Engineering
University of Rochester
Rochester, NY, USA
selcuk.kose@rochester.edu

Mehmet E. Belviranli

Computer Science Department
Colorado School of Mines
Golden, CO, USA
belviranli@mines.edu

Abstract—Shared-memory system-on-chips (SM-SoC) are ubiquitously employed by a wide-range of mobile computing platforms, including edge/IoT devices, autonomous systems and smartphones. In SM-SoCs, system-wide shared physical memory enables a convenient and financially-feasible way to make data accessible by dozens of processing units (PUs), such as CPU cores and domain specific accelerators. In this study, we investigate vulnerabilities that stem from the shared use of physical memory in such systems. Due to the diverse computational characteristics of the PUs they embed, SM-SoCs often do not employ a shared last level cache (LLC). While the literature proposes covert channel attacks for shared memory systems, high-throughput communication is currently possible by either relying on an LLC or privileged/physical access to the shared memory subsystem.

In this study, we introduce a new memory-contention based covert communication attack, MC^3 , which specifically targets the shared system memory in mobile SoCs. Different from existing attacks, our approach achieves high throughput communication between applications running on CPU and GPU without the need for an LLC or elevated access to the system. We extensively explore the effectiveness of our methodology by demonstrating the trade-off between the channel transmission rate and the robustness of the communication. We demonstrate the utility of MC^3 on NVIDIA Orin AGX, Orin NX, and Orin Nano up to a transmit rate of 6.4 kbps with less than 1% error rate.

I. INTRODUCTION

Mobile system-on-chips (SoC) house multiple types of processing units (PUs), including general-purpose CPU cores and domain specific accelerators (DSAs), such as GPUs and neural network accelerators. With the proliferation of integrated DSAs, modern SoCs can provide cost effective and energy-efficient execution, making them ideal candidates for in-the-field computing in many areas (mobile phones [37], smart home environments [17] and autonomous systems [26]). An emerging architectural feature of such SoCs (i.e., NVIDIA’s Orin [26], Apple’s M3 [2], Qualcomm’s Snapdragon [30], Coral Dev Board [6]) is a shared main memory where the data is stored

This paper is accepted to 2025 Design, Automation & Test in Europe Conference & Exhibition (DATE).

for access by all PUs, including CPUs and DSAs, in system.

The use of shared physical memory (SM) in commodity SoCs is motivated by the goal of reducing chip area and production costs. Unlike discrete memory architectures, where each different type of PU operates on its own private memory, the use of SMs in SoCs can also provide additional performance benefits by minimizing data transfer overhead between system CPU and accelerators [9], [8]. SM-SoCs also lack a shared last level cache (LLC) to avoid complex per-PU design requirements to support cache-coherency and shared virtual memory addressing. As a result, when running multiple workloads concurrently, PUs in SM-SoCs can experience significant slowdown caused by shared memory contention [38], [16], [22], [7].

Over the years, security researchers showed that having a shared hardware component with a predictable slowdown behavior leaves a unique fingerprint that could be leveraged to implement various attacks [21], [34], [40]. Covert-channel communication attacks that target the vulnerabilities in the memory subsystem can be categorized into three: (1) *Cache-based, high-throughput attacks* which leverage the LLC between high-performance CPU cores [21], [39], [13], ARM cores on mobile systems [20], [5], between cores of a GPU [11] or between CPU and GPU [10]. (2) *Low-throughput attacks targeting directly the DRAM* rely on memory performance attacks [32], memory de-duplication [4], [36], bus snooping [40] and monitoring DRAM power consumption [28]. (3) *Attacks requiring elevated privileges or HW access* [29], [23], [32], [31]. None of these works cumulatively addresses the constraints required by our threat model (See Section III).

Constructing a fine-grained, low-noise, and high-throughput memory-contention-based covert channel attack on mobile SM-SoCs, presents several challenges: (i) In the absence of LLCs, the trojan (i.e., transmitter) needs to generate sufficient memory pressure that is observable by the spy (i.e., receiver). CPU-based workloads in resource limited SM-SoCs often fail to

utilize the memory bandwidth fully even when all the cores are used. Therefore, high-memory-demanding accelerators such as GPUs should be utilized. (ii) The memory system pressure exerted cumulatively by the spy and the trojan needs to be high enough to be reliable but also low enough to minimize the risk of being detected by system defenses. This is crucial to maximize the communication channel's capacity and maintain the stealthiness of the attack. (iii) Without external synchronization mechanisms, reliable & high-throughput data transmission over SM becomes challenging, as the trojan and spy may operate at different magnitudes of memory operations when located and different type of PUs (e.g., CPU cores and the GPU). (iv) These requirements should be achieved without the need for elevated privileges and HW access, and the attack should work under single-user & multi-application environments. Our proposed work tackles all of the four challenges listed above.

In this paper, we introduce a new memory contention-based covert communication attack, MC^3 , targeting shared memory SoCs on mobile platforms. Our attack exploits the underlying vulnerability with software-only mechanisms without the need for direct access to the HW or super-user privileges. Our approach is designed to achieve a fine balance between the communication accuracy and the transmission rate (*i.e.*, capacity) of the covert channel. To increase the transmission rate and improve the efficiency of our attack, we further propose a CPU+GPU version of the receiver and the transmitter. We demonstrate the capabilities of our attack by showing that it achieves transmission rates of up to 6.4 kbps with an error rate of less than 1% on CPU to GPU communication.

Our work makes the following contributions:

- We unveil a new attack vector based on shared memory contention visible via software-only measurements and requiring no privileged access to the system.
- We introduce a novel covert channel attack methodology, called memory contention based covert communication, that targets shared memory in SM SoCs.
- We present a new class of transmitter- and receiver-based attack that can utilize either both CPU and GPU or only CPU within a shared memory system. Our attack is evaluated under basic user-level privilege and does not have access to any hardware component requiring elevated permission.
- We demonstrate the utility of MC^3 on NVIDIA Orin AGX, Orin Nano, and Orin NX reaching up to channel capacity of 6.4 Kbps with 95% accuracy or 1.3 Kbps with 99.99%.

II. BACKGROUND

A. Shared Memory SoCs (SM-SoC)

Modern SoCs, such as NVIDIA's Xavier and Orin architectures (as depicted in Fig. 1), Apple's M and Bionic series, and Qualcomm's Snapdragon 8 series, integrate dozens of accelerators, such as GPUs and neural processing units, and each is optimized to perform specific operations very efficiently. Different from larger-scale systems where each accelerator has a dedicated primary memory, accelerators, and CPUs, SM-SoCs share a common DRAM-based architecture such as DDR4. Each PU accesses to the memory via a shared memory bus and a centralized memory controller (MC). Due to their inherent

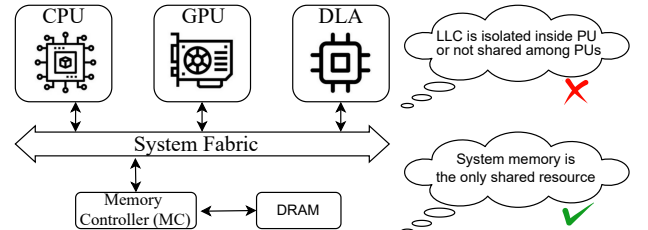


Fig. 1: Block diagram for NVIDIA's Xavier AGX SoC embedding multiple PUs on a single shared memory subsystem.

architectural heterogeneity [38], SM-SoCs often lack a shared LLC. Modern SoCs benefit from shared-memory design in three distinct ways:

- Many SoCs are area-limited due to devices they are integrated into such as mobile phones, edge devices, and laptops.
- Multiple PUs (*i.e.*, CPU and GPU) can effectively transfer data among each other by eliminating the data copies needed for discrete memory designs.
- Reducing production cost of such devices since billions of each are produced every year.

B. Additional Related Work

Denial-of-service (DoS) attacks [25], [39] exhaust the memory subsystem and cause a significant increase in memory access latencies. Commonly deployed memory controller (MC) scheduling policies, such as fairness control [12] and adaptive scheduler [19], often designed to maximize system's performance. Security-prioritized MC schedulers [33], [35] target to prevent such memory performance attacks with limited overhead, yet still not able to completely eliminate the threat. Our work focuses on covert-channel communication, which requires a much higher level of precision than DoS attacks.

There are also other researches studying architectural covert channels in the cloud [40], [39], HPC servers [11], and desktops [24], [15]. Similar studies also leveraged temperature [34], [14] and power [18], [34] as the covert communication channel. Our work focuses on the vulnerabilities stemming from shared memory use.

III. THREAT MODEL

Figure 2 illustrates our threat model, involving two (or more) applications running on an SM-SoC with no shared LLC across the PUs (as explained in Section II-A). Applications are assumed to be developed by third-party vendors and installed via an application store that the underlying platform, such as a smart home system, provides. Transmitter (*i.e.*, trojan) is an application that has access to sensitive/private user data. User-controlled permissions are assumed to grant the trojan to access such data. The receiver (*i.e.*, spy) is an application running on the same SM-SoC but does not have any means to access the sensitive/private data. Applications running in the system (including receiver and transmitter) are not allowed to communicate with each other. Transmitter and receiver run on the CPU and the GPU (in no specific order) with no elevated execution privileges (*e.g.*, they cannot access protected OS facilities or performance counters). The attacker is assumed to have no physical access to the HW components and therefore cannot directly measure physical leakage such as power consumption

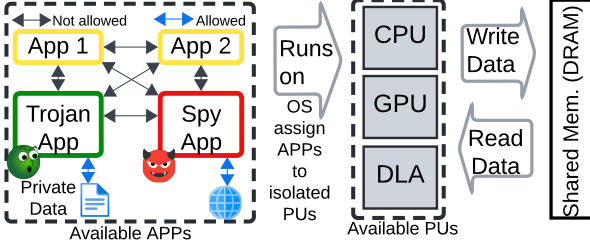


Fig. 2: Threat Model

and electromagnetic emanations. The attack is designed to be executed remotely, without the need for the attacker to be near the target device or to actively engage during the attack's execution.

IV. SHARED MEMORY CONTENTION BASED ATTACK VECTOR (SMCAV)

Our proposed methodology relies on the vulnerability we discover in shared memory SoCs and has the potential to be exploited on mobile and autonomous SoCs for a variety of attacks without a need for privileged or HW access. A programmer can develop the adversary transmitter application to leave a meaningful shared memory access signature. This memory signature can leak any crucial information that can be encoded as binary from the adversary receiver application.

Although this attack strategy seems similar to other type of covert channel attacks, there are unique challenges to efficiently and reliably designing shared memory contention channels:

- *Sufficiently observable contention:* While fully stressing memory resources to maximize contention is technically possible by the use of accelerators, designing attack vectors to generate sufficiently observable contention for the transmitter and contention sensing for the receiver will not only help the attack to remain undetected by counter measures deployed by the OS but can also increase the channel capacity of the attack. On the other hand, low utilization of memory resources may not cause enough contention, leading the receiver not to observe contention reliably. We deal with this challenge by creating a contention that only targets shared memory resources and bypasses the private cache hierarchy of CPUs.
- *Reliable and efficient contention:* Achieving reliable contention generation necessitates a careful characterization of the channel's behavior. While reliability can be increased by repetitively performing contention for a long time to transmit a bit, the practicality of the attack often requires minimizing the repetition. We overcome these challenges by deeply analyzing the contention behavior (*i.e.*, adjusting the delay time to contention effect starts being observed and *i.e.*, minimizing the effect of contention being accumulated) by using fine-grained time intervals for the receiver and the transmitter.
- *Matching communication rate of transmitter and receiver:* Unlike traditional cache attacks where a cache hit-miss effect can be observed clearly in orders of nanoseconds, the slowdown under memory contention becomes visible in microseconds, requiring matching transmitter and receiver time intervals. On the other hand, considering computational capability and clock rate differences of a CPU and GPU in a system, the design of attack vectors on two completely

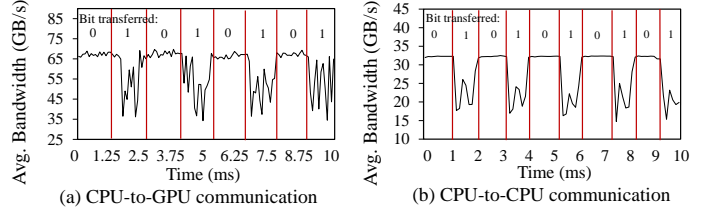


Fig. 3: Raw traces for CPU-to-CPU and CPU-to-GPU via SM contention channel

different PUs requires to sync both receiver and transmitter without using any external resources. We overcome this challenge by developing a precise contention generator and sleep for transmitter and adapting the receiver accordingly.

Feasibility of shared memory contention based communication channel: To demonstrate how the memory contention behavior affects the observed bandwidth of an application, we set the transmitter app to run on CPU whereas we test the receiver on both CPU and GPU on Orin NX. Fig. 3 shows two raw traces of varying average bandwidth (BW) perceived on the receiver side. Regardless of whether the receiver runs on CPU or GPU, the perceived BWs for the receiver have clear drops in the traces which correspond to the '1's sent by the transmitter. This experiment demonstrates the feasibility of building covert channels with shared memory contention.

V. MC³: SHARED MEMORY CONTENTION BASED COVERT CHANNEL COMMUNICATION

A. Overall Mechanism

Fig. 4 illustrates the communication protocol between the transmitter and receiver for transmitting bits (*i.e.*, 0 or 1) through shared memory contention. The transmitter conveys bits by performing buffer copy operations on memory while the receiver continuously performs another buffer copy operation to detect the transmitted bit.

The transmitter is responsible for sending the bit by modulating the level of memory contention via copy operation with a predetermined amount of buffer size. As shown in the upper part of Fig. 4, to transmit a bit '0', the transmitter sleeps for a predefined time interval of T_n . To send a bit '1', it performs continuous copy operations to access DRAM. The receiver continuously operates its own buffer copy function, then measures the latency of buffer copy operation and calculates the average BW over the time interval, which will be used to determine the value of the received bit.

As illustrated in the below part in Fig 4, when transmitter sleeps, the receiver can perform more copy operations with low latency (*i.e.*, high memory BW) during the time interval T_n . Multiple copy operations per interval can be also used to have more reliable data transmission. Conversely, when transmitter creates a contention by performing a copy operation, the receiver's throughput decreases (*i.e.*, low memory BW) because memory latency increases due to shared memory contention.

While running the receiver non-stop is possible, we opt to start the receiver slightly earlier (*e.g.*, one second) than the transmitter at a predetermined timestamp. This design eliminates the need for continuous operation of the receiver, thereby minimizing the chance of our attack being detected under real-

TABLE I: Targetted experiment platforms

Device	Orin AGX	Orin Nano	Orin NX
CPU	12-core A78 ARM	6-core A78AE ARM	8-core A78AE ARM
GPU	2048 core Ampere	1024 core Ampere	1024 core Ampere
DRAM & BW	64 GB 256-bit 204.8 GB/s	8 GB 128-bit 68 GB/s	8 GB 128-bit 102 GB/s

life conditions. The reason for the early start is to collect average BW (latency per copy operation) for the receiver under no contention by transmitter, which can be used as a baseline during the data analysis stage. Although other applications on the device may use shared memory —potentially introducing noise in receiver’s average BW measurements—the pattern of zeros and ones can be detected using heuristic history-based signal processing approaches.

Table I lists our testing devices with varying computational capability and memory BW capacity in each device. We use Jetpack 5.1 on all devices. It is worth noting that all devices have TrustZone trusted execution environment (TEE) and OS-protection regions in the memory subsystem.

B. Attack Vector

Our attack leverages a memory-contention channel to covertly transmit data between a transmitter and a receiver.

Our transmitter algorithm is briefly explained in Alg.1. It is responsible for encoding the data and transmitting the encoded data bitstream over the memory-contention channel. It works by looping over the input data bitstream and either runs the memory contention kernel (*i.e.*, data copy operation) over the time interval T if the current bit is a 1, resulting in memory contention, or sleeps over the same time interval (if not set differently) T if the current bit is a 0, resulting in near zero memory contention.

Our receiver algorithm is explained in Alg. 2. It is responsible for receiving the encoded data over the memory-contention channel and decoding it. It works by continuously running the memory contention kernel over the time interval T (T value is designed to be the same as the transmitter is using). Then, it normalizes the BWs based on a global average (*i.e.*: subtracts each BW sample from the overall average observed BW) [40]. Then, this normalized BW is thresholded (with hysteresis, which we experimentally determined to be much more resistant to noise). Finally, the result of this thresholding is converted directly into the received bitstream, where values above the threshold are a 0 (which corresponds to a higher measured BW on the receiver, as a result of the transmitter **not** simultaneously generating memory contention) and values below the additive inverse (*i.e.*: $-1 \times$) of the threshold are a 1 (which corresponds to a lower measured BW on the receiver, as a result of the

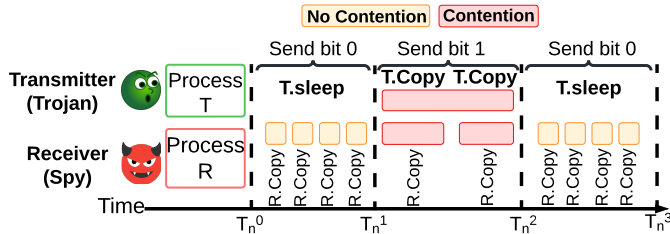


Fig. 4: Overview: communication between sender and receiver.

Algorithm 1 Transmitter

```

Input: data bitstream  $B$  and its length  $n$ , time interval  $T$ 
for  $i \leftarrow 0$  to  $n - 1$  do
    if  $B[i]$  is 1 then CONTEND_FOR( $T$ )     $\triangleright$  Generate contention
    else SLEEP_FOR( $T$ )                   $\triangleright$  Remain idle

```

Algorithm 2 Receiver

```

Input: hysteresis threshold  $\gamma$ , run length  $n$ , time interval  $T$ 
 $B \leftarrow []$                                  $\triangleright$  Output bitstream (starts empty)
 $b \leftarrow 0$                                  $\triangleright$  Hysteresis state
 $\bar{\beta} \leftarrow 0$                              $\triangleright$  Average BW
for  $i \leftarrow 0$  to  $n - 1$  do
     $\beta_{\text{raw}} \leftarrow \text{CONTEND\_FOR}(T)$ 
     $\beta = \frac{\bar{\beta} \cdot i + \beta_{\text{raw}}}{i + 1}$            $\triangleright$  Use simple global average
     $\beta_{\text{normalized}} = \beta_{\text{raw}} - \bar{\beta}$ 
    if  $\beta_{\text{normalized}} > \gamma$  then APPEND( $B$ , 0)
         $b \leftarrow 1$ 
    else if  $\beta_{\text{normalized}} < (-1 \cdot \gamma)$  then APPEND( $B$ , 1)
         $b \leftarrow 0$ 
    else APPEND( $B$ ,  $b$ )
return  $B$ 

```

transmitter simultaneously generating memory contention).

C. Cache-less Memory Access

Throughout the development of the memory-contention kernel, we’ve observed that CPU caches can be used to access the data and artificially inflate memory BW measurements (since cache is much faster than DRAM), making our BW measurements unreliable and introducing substantial noise into the communication channel. Considering that our goal is to create contention in DRAM, performing read/write operations utilizing the cache can also diminish the effectiveness of the attack.

To alleviate this, our implementation employs memory instructions with non-temporal hints, specifically `ldnp/stnp` (Load/Store Pair Non-Temporal) Arm64 instructions. This hint represents the data being loaded or stored is unlikely to be reused soon, prompting the system to bypass the cache hierarchy [1]. By doing so, we ensure that our memory operations access DRAM directly, enhancing the reliability of our BW measurements and increasing the efficiency of the attack. It is worth noting that we observed sufficient contention generation with data streaming using regular data streaming without non-temporal instructions.

D. Precise Contention Duration and Precise Sleep

In order to maximize performance, the sleep and data copy operations require high temporal precision (*i.e.*: sleep or run for the desired duration as accurately as possible). We implemented a precise sleep mechanism by utilizing an OS-provided function (*i.e.*: `std::this_thread::sleep_for`) until near the desired end time and finally spinning (*i.e.*: while loop with an empty body) until the desired end time is achieved [3]. To implement `CONTEND_FOR(T)`, used in both algorithms, our

TABLE II: Precise contention generation and sleep for

Operation	Expected duration	Mean Error	Minimum Error	Maximum Error	Std. dev. Error
Sleep for	100 ms	46 ns	5 ns	314 ns	41 ns
Contention	100 ms	12 μ s	5 ns	767 μ s	65 μ s

data copy operation first runs the memory-contention kernel for a small, fixed amount of data (*i.e.*, taking nearly one second) to estimate the current achievable memory contention BW (β_0). Using the total desired duration (T), it estimates the amount of data the kernel needs to run for (d_* , where $d_* \propto \beta_0 \cdot T$). Using this estimate, it splits this total data estimate up (*e.g.*: $d_i = \frac{1}{100} \cdot d_*$), run the memory-contention kernel (for d_i amount of data), collect β_i , update d_* and d_i , and repeat. When it gets close to the desired end time, it further splits up the estimate (*e.g.*: $d_i = \frac{1}{1000} \cdot d_*$) to reduce the amount of under/overshoot. In Table II, we represent the results for 100 ms execution, demonstrating our average error rate of 4 and 7 orders of magnitude lower for sleep and contention generation, respectively.

E. Transmitter and Receiver Design

Our attack hinges on the transmitter generating sufficient memory requests to create noticeable contention, which the receiver must detect. Essentially, the transmitter needs to generate enough data requests to contend with the receiver, and the receiver must be sensitive enough to observe the difference between the transmitter's sleep and data copy operations. To evaluate this, we conducted experiments on Orin Nano using three CPU cores for both transmitter and receiver. We send 1024-bit information evenly distributed with bit 0s and 1s, with the slowdown results illustrated in Fig 5.a. We design varying buffer sizes of data copy for transmitter (from 0.6 MiB to 128 MiB) and receiver (from 1 MiB to 100 MiB). Overall, we observe an increasing pattern of average slowdown in receiver side as we increase transmitter buffer sizes. For instance, with a 1 MiB buffer size for the receiver, the transmitter requires at least a 2 MiB buffer (*i.e.*, at least 20% MC utilization) to achieve a minimum of 10% slowdown. This level of slowdown enables the receiver to clearly distinguish between contention (bit '1') and no-contention (bit '0') states.

We also sense the slowdown on receiver to demonstrate the slowdown differences between bit '1' and bit '0'. To demonstrate this, we measure and analyze the average BW perceived on receiver side while transmitter, having 4 MiB buffer size, sends bit '0' (High) and bit '1' (Low). Fig. 5.b demonstrates the distribution (including outliers) of perceived BW by receiver while sensing 0s (light colors) and 1s (dark colors). Even though buffer sizes of 1.6 and 1.0 MiB have clear differences in terms of perceived BW, lower buffer sizes for receiver fail to distinguish the differences between bit '0' and '1' by looking into perceived BW. While outliers create noises if accuracy is calculated solely with average-based methods, history-based (comparing the current trace with the previous) methods clearly identify the changes. Even though transmitter with 0.8 MiB design has approximately 10% MC utilization, the contention may not be enough to distinguish the bit 0s and 1s.

F. Trade-off between Time and Contention Amount

The channel capacity intuitively depends on the size of the transmitter's buffer being copied. Assuming that (to transmit bit '1') transmitter copy operation with a fixed buffer size will be performed once during time interval T_n , there exists an inverse relationship between the transmitter buffer size and the channel capacity, as demonstrated in Eq. 1. As we increase

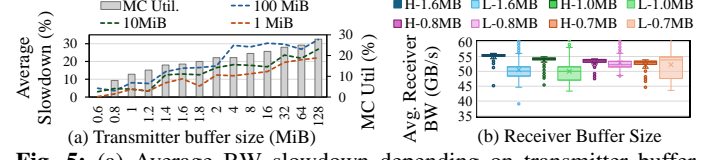


Fig. 5: (a) Average BW slowdown depending on transmitter buffer size. (b) Average perceived BW depending on receiver size for low (L) and high (H), respectively for bit 0 and bit 1.

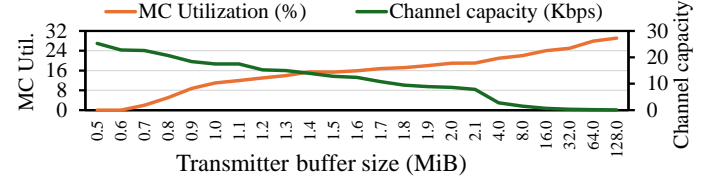


Fig. 6: MC utilization per transmitter buffer size

transmitter buffer size, thus time to a copy operation of a buffer $Time_{Tra}$ and account for the average slowdown by receiver $Slowdown_{Rec}$, the channel capacity decreases.

$$Channel Capacity = 1/(Time_{Tra} * Slowdown_{Rec}) \quad (1)$$

Ideally, we aim to use the smallest possible transmitter buffer size to maximize the channel capacity of our covert channel. On the other hand, there is a lower limit to how much we can decrease the buffer size to generate observable contention. To empirically demonstrate the trade-off between channel capacity and the buffer size, we performed experiments by increasing the transmitter's buffer size, as shown in Fig. 6. We observe that increasing the transmitter buffer size leads to a nearly linear decrease in channel capacity. For example, with transmitter buffer sizes of 0.5 MiB and 0.6 MiB, we achieved channel capacities of up to 15 kbps, yet the receiver was unable to detect the transmitter's activity since transmitter's MC utilization was nearly zero.

G. Reducing Noise

Synchronization of transmitter and receiver is essential for accurately sensing BW differences. Since direct communication between the transmitter and receiver is not allowed, we should statically decide the time intervals. Yet, as depicted by Fig. 5.b, due to the nature of generating contention being noisy, the accumulation of errors with outliers can lead to an out-of-sync operation. If we target to operate in worst case scenario, then many contended regions may complete earlier than anticipated.

We illustrate ideal and realistic execution scenarios as depicted in Fig. 7 under (T)ransmitter/(R)eceiver=1 configuration. So, instead of targeting one-to-one overlap, we design to have multiple perceived average BW by the receiver per transmitter.

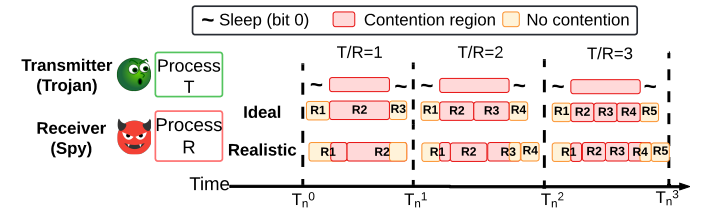


Fig. 7: Overlapping time between transmitter and receiver copies

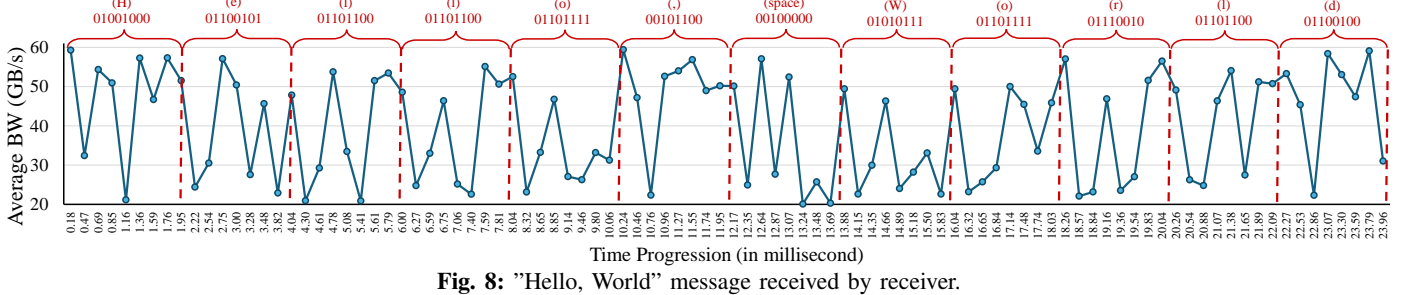


Fig. 8: "Hello, World" message received by receiver.

For scenarios where R1 and R2 overlap with the same transmitter, leading to perceiving less BW for both R1 and R2 even though only one bit '1' is transferred. However, even though transmitter and receiver get out of sync, T/R=2 scenario can capture at least one full-contended region. While this might reduce channel capacity by half (if the receiver will have a fixed data copy operation), this approach can significantly increase the accuracy of our channel by eliminating noise.

Receiver collects more traces while transmitter sleeps since no contention occurs. To optimize channel capacity, we observe that the longer time interval can be statically pre-determined for contention generation compared to sleep.

VI. UTILIZING ACCELERATORS TO IMPROVE CHANNEL CAPACITY

Mobile and autonomous SoCs integrate more GPUs and additional accelerators for domain-specific workloads. Given the high computation capabilities of GPUs, they can generate more data requests from memory than CPUs.

A. Receiver on GPU

As explained in earlier sections, sensitivity of receiver is crucial for distinguishing between bit '0' and '1'. Thus, we target to run receiver on GPU and transmitter on CPU. We implemented memory copy application via `cudaMemcpy` on CUDA [27]. We depict the average slowdown of receiver for bit '0' (i.e., High) and '1' (i.e., Low) from transmitter using a buffer size of 1 MB on Orin AGX in Fig 9.a. From 2MB to 8MB data size, we observe a clear difference between bit 1s and 0s. Buffer sizes of 0.5MB and 1MB do not sense the contention enough whereas we observe timing intervals for 16MB or higher may not align properly due to high T/R ratio as explained in 7. We also experimented with configuring transmitter on GPU and receiver on CPU, yet we observed worse quality of sensitivity demonstrating the difference 0s and 1s compared to receiver on GPU and results are omitted due to space limitations.

B. Receivers Capacity on GPU and CPU

Having more traces of perceived BW per transmitted data can improve the accuracy of the attack vector. To further analyze the receiver on CPU and GPU, we performed an experiment to compare the number of traces generated per millisecond and

their average slowdown on Orin AGX. The results are depicted in Fig 9.b. We observe that we can generate up to 14k and 5k traces with 9% and 7% slowdowns on GPU and CPU, respectively. As we increase buffer sizes, we observe fewer traces but more contention per trace on average in both CPU and GPU. It is worth noting that we use 11 and 6 cores on the transmitter with receivers on GPU and CPU, respectively, since we can allocate more CPU cores to the transmitter without a significant need to split for receiver. This also increases transmitter contention generation capability. Overall, we observe 3x-5x and 2x-4x channel capacity increase when we use GPUs instead of CPUs in Orin AGX and Orin Nano, respectively.

C. Hello World Transmission

To assess our design's performance with longer messages, we transmitted a 100 Kb text message on Orin Nano. The results are depicted in Fig. 8. Y-axis shows the average perceived BWs (calculated by taking the average of two traces per time interval) during each time interval whereas X-axis is the time progression in milliseconds. We highlight the beginning of the message reading "Hello, World" with 100% accuracy and the entire message with 99.02% accuracy at an over 4 Kbps channel rate. We evaluate accuracy as explained in Sec. V-B.

D. Channel Capacity vs Accuracy on CPU-to-GPU

We further demonstrate trade-off between channel capacity and accuracy when we utilize GPU as receiver on Orin AGX. Fig. 10.a and Fig. 10.b present the results for varying transmitter and receiver buffer sizes as we gradually increased the channel capacity starting from approximately 500 while transmitting a 16 Kb message. In Fig. 10.a, we adjusted the transmitter buffer sizes while keeping the receiver buffer size fixed at 1 MB. The increase in channel capacity was achieved by varying the number of buffer copy operation iterations per time interval from 1 to 10, adjusting the receiver accordingly. Overall, our results demonstrate up to 6.4 Kbps capacity or up to 99.99% accuracy. As the transmitter buffer size and number of buffer iterations per interval increased, we observed higher accuracy but a reduction in channel capacity. For instance:

- 2MB transmitter achieved capacity of 3.5 Kpbs with 99.1%

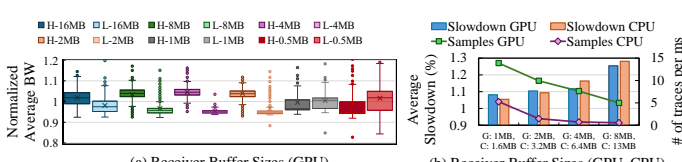


Fig. 9: (a) Perceived BW distribution depending on receiver size for low and high on GPU. (b) Average BW slowdown and number of traces per millisecond generated by receiver on (C)PU and (G)PU.

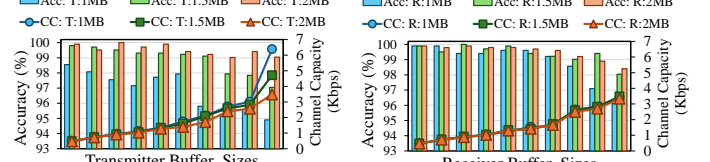


Fig. 10: Varying transmitter and receiver buffer sizes demonstrating the effect on the trade-off between (Acc)curacy and channel capacity (CC).

accuracy and 1.3 Kpbs with near-perfect accuracy of 99.99%.

- 1MB transmitter achieved capacity of 6.4 Kpbs with 94.9%.

In Fig. 10.b, we kept transmitter buffer size (1 MB) and iteration of receiver per transmitter (*i.e.*, T/R ratio) constant, but increased receiver buffer size and buffer copy operation iterations of transmitter per interval. Overall, increasing the receiver buffer size (when transmitter copy iteration is the same) enhanced accuracy with minimal impact on channel capacity up to a certain point. It is worth noting that increasing receiver size degrades the accuracy since T/R ratio becomes unbalanced, which we observe as 5 MB in this configuration. Similar to the observations in Fig. 10.a, increasing the channel capacity by operating transmitter operation per interval led to a decrease in accuracy.

VII. CONCLUSION

In conclusion, we have demonstrated *MC*³, a novel and efficient covert channel attack exploiting shared memory contention in SM-SoCs without requiring privileged access. Our methodology achieves kpbs-level transmission rates by using CPU and GPU or only CPU with less than 1% error rates, highlighting a significant security vulnerability in modern shared-memory mobile platforms.

REFERENCES

- [1] Arm® Architecture Reference Manual for A-profile architecture, 2024.
- [2] Apple. Apple unveils the new macbook pro featuring the m3 family of chips, 2023. (accessed on 09/22/2024).
- [3] Blat Blatnik. The perfect Sleep() function. <https://blog.bearcats.nl/perfect-sleep-function/>.
- [4] Erik Bosman, Kaveh Razavi, Herbert Bos, and Cristiano Giuffrida. Dedup est machina: Memory deduplication as an advanced exploitation vector. In *2016 IEEE symposium on security and privacy (SP)*, pages 987–1004. IEEE, 2016.
- [5] Yun Chen, Arash Pashtashid, Yongzheng Wu, and Trevor E Carlson. Prime+ reset: Introducing a novel cross-world covert-channel through comprehensive security analysis on arm trustzone. In *2024 Design, Automation & Test in Europe Conference & Exhibition (DATE)*, pages 1–6. IEEE, 2024.
- [6] Coral. Dev board. <https://coral.ai/products/dev-board/>, 2024. (accessed on 09/22/2024).
- [7] Ismet Dagli and Mehmet E Belviranli. Shared memory-contention-aware concurrent dnn execution for diversely heterogeneous system-on-chips. In *Proceedings of the 29th ACM SIGPLAN Annual Symposium on Principles and Practice of Parallel Programming (PPoPP'24)*, pages 243–256, 2024.
- [8] Ismet Dagli, Alexander Cieslewicz, Jedidiah McClurg, and Mehmet E Belviranli. Axonn: Energy-aware execution of neural network inference on multi-accelerator heterogeneous socs. In *DAC*, pages 1069–1074, 2022.
- [9] Mohammad Dashti and Alexandra Fedorova. Analyzing memory management methods on integrated cpu-gpu systems. In *Proceedings of the 2017 ACM SIGPLAN International Symposium on Memory Management (ISMM)*, pages 59–69, 2017.
- [10] Sankha Baran Dutta, Hoda Naghibijouybari, Nael Abu-Ghazaleh, Andres Marquez, and Kevin Barker. Leaky buddies: Cross-component covert channels on integrated cpu-gpu systems. In *2021 ACM/IEEE 48th Annual International Symposium on Computer Architecture (ISCA)*, pages 972–984. IEEE, 2021.
- [11] Sankha Baran Dutta, Hoda Naghibijouybari, Arjun Gupta, Nael Abu-Ghazaleh, Andres Marquez, and Kevin Barker. Spy in the gpu-box: Covert and side channel attacks on multi-gpu systems. In *Proceedings of the 50th Annual International Symposium on Computer Architecture (ISCA)*, pages 1–13, 2023.
- [12] Eiman Ebrahimi, Chang Joo Lee, Onur Mutlu, and Yale N Patt. Fairness via source throttling: a configurable and high-performance fairness substrate for multi-core memory systems. *ACM Sigplan Notices*, 45(3):335–346, 2010.
- [13] Aditya S Gangwar, Prathamesh N Tanksale, Shirshendu Das, and Sudeepa Mishra. Flush+ early reload: Covert channels attack on shared l1c using mshr merging. In *2024 Design, Automation & Test in Europe Conference & Exhibition (DATE)*, pages 1–6. IEEE, 2024.
- [14] Jeferson González-Gómez, Kevin Cordero-Zuñiga, Lars Bauer, and Jörg Henkel. The first concept and real-world deployment of a gpu-based thermal covert channel: Attack and countermeasures. In *2023 Design, Automation & Test in Europe Conference & Exhibition (DATE)*, pages 1–6. IEEE, 2023.
- [15] Marc Green, Leandro Rodrigues-Lima, Andreas Zankl, Gorka Irazoqui, Johann Heyszl, and Thomas Eisenbarth. {AutoLock}: Why cache attacks on {ARM} are harder than you think. In *26th USENIX Security Symposium (USENIX Security 17)*, pages 1075–1091, 2017.
- [16] Mark Hill and Vijay Janapa Reddi. Gables: A roofline model for mobile socs. In *2019 IEEE International Symposium on High Performance Computer Architecture (HPCA)*, pages 317–330. IEEE, 2019.
- [17] Ahmad Jalal, Majid Ali Khan Quaid, and Kibum Kim. A wrist worn acceleration based human motion analysis and classification for ambient smart home system. *Journal of Electrical Engineering & Technology*, 14:1733–1739, 2019.
- [18] S Karen Khatamifard, Longfei Wang, Amitabh Das, Selcuk Kose, and Ulya R Karpuzcu. Powert channels: A novel class of covert communicationexploiting power management vulnerabilities. In *2019 IEEE International Symposium on High Performance Computer Architecture (HPCA)*, pages 291–303. IEEE, 2019.
- [19] Yoongu Kim, Dongsu Han, Onur Mutlu, and Mor Harchol-Balter. Atlas: A scalable and high-performance scheduling algorithm for multiple memory controllers. In *HPCA-16 2010 The Sixteenth International Symposium on High-Performance Computer Architecture (HPCA)*, pages 1–12. IEEE, 2010.
- [20] Moritz Lipp, Daniel Gruss, Raphael Spreitzer, Clémentine Maurice, and Stefan Mangard. {ARMageddon}: Cache attacks on mobile devices. In *25th USENIX Security Symposium (USENIX Security 16)*, pages 549–564, 2016.
- [21] Fangfei Liu, Yuval Yarom, Qian Ge, Gernot Heiser, and Ruby B Lee. Last-level cache side-channel attacks are practical. In *2015 IEEE symposium on security and privacy (S&P)*, pages 605–622. IEEE, 2015.
- [22] Hao Luan, Yu Yao, and Chang Huang. A many-ported and shared memory architecture for high-performance adas socs. *IEEE Design & Test*, 39(6):5–15, 2022.
- [23] Yang Luo, Wu Luo, Xiaoning Sun, Qingni Shen, Anbang Ruan, and Zhonghai Wu. Whispers between the containers: High-capacity covert channel attacks in docker. In *2016 IEEE trustcom/bigdata/ispa*, pages 630–637. IEEE, 2016.
- [24] Nikolay Matyunin, Nikolaos A Anagnostopoulos, Spyros Boukopoulos, Markus Heinrich, André Schaller, Maksim Kolinichenko, and Stefan Katzenbeisser. Tracking private browsing sessions using cpu-based covert channels. In *Proceedings of the 11th ACM Conference on Security & Privacy in Wireless and Mobile Networks (WiSeC)*, pages 63–74, 2018.
- [25] Thomas Moscibroda Onur Mutlu. Memory performance attacks: Denial of memory service in multi-core systems. In *USENIX security*, 2007.
- [26] NVIDIA. Next-level ai performance for next-gen robotics — nvidia jetson orin agx. <https://www.nvidia.com/en-us/autonomous-machines/embedded-systems/jetson-orin/>, 2023. (accessed on 09/22/2024).
- [27] NVIDIA. Cuda samples. https://github.com/NVIDIA/cuda-samples/tree/master/Samples/1_Utils/bandwidthTest, 2024. (accessed on 09/22/2024).
- [28] Thales Bandiera Paiva, Javier Navaridas, and Routh Terada. Robust covert channels based on dram power consumption. In *Information Security: 22nd International Conference, ISC 2019, New York City, NY, USA, September 16–18, 2019, Proceedings 22*, pages 319–338. Springer, 2019.
- [29] Peter Pessl, Daniel Gruss, Clémentine Maurice, Michael Schwarz, and Stefan Mangard. {DRAM}: Exploiting {DRAM} addressing for {Cross-CPU} attacks. In *25th USENIX security symposium (USENIX security 16)*, pages 565–581, 2016.
- [30] Qualcomm. Snapdragon mobile platforms. <https://www.qualcomm.com/snapdragon/products>, 2024.
- [31] Michael Schwarz, Moritz Lipp, Daniel Moghimi, Jo Van Bulck, Julian Stecklina, Thomas Prescher, and Daniel Gruss. Zombieload: Cross-privilege-boundary data sampling. In *Proceedings of the 2019 ACM SIGSAC Conference on Computer and Communications Security (ASIACCS)*, pages 753–768, 2019.
- [32] Michael Schwarz, Clémentine Maurice, Daniel Gruss, and Stefan Mangard. Fantastic timers and where to find them: High-resolution microarchitectural attacks in javascript. In *Financial Cryptography and Data*

Security: 21st International Conference, FC 2017, Sliema, Malta, April 3-7, 2017, Revised Selected Papers 21, pages 247–267. Springer, 2017.

- [33] Ali Shafiee, Akhila Gundu, Manjunath Shevgoor, Rajeev Balasubramonian, and Mohit Tiwari. Avoiding information leakage in the memory controller with fixed service policies. In *Proceedings of the 48th International Symposium on Microarchitecture (MICRO)*, pages 89–101, 2015.
- [34] Hritvik Taneja, Jason Kim, Jie Jeff Xu, Stephan Van Schaik, Daniel Genkin, and Yuval Yarom. Hot pixels: Frequency, power, and temperature attacks on {GPUs} and arm {SoCs}. In *32nd USENIX Security Symposium (USENIX Security 23)*, pages 6275–6292, 2023.
- [35] Yao Wang, Andrew Ferraiuolo, and G Edward Suh. Timing channel protection for a shared memory controller. In *HPCA*, pages 225–236. IEEE, 2014.
- [36] Jidong Xiao, Zhang Xu, Hai Huang, and Haining Wang. Security implications of memory deduplication in a virtualized environment. In *2013 43rd Annual IEEE/IFIP International Conference on Dependable Systems and Networks (DSN)*, pages 1–12. IEEE, 2013.
- [37] Yunyang Xiong, Hanxiao Liu, Suyog Gupta, Berkin Akin, Gabriel Bender, Yongzhe Wang, Pieter-Jan Kindermans, Mingxing Tan, Vikas Singh, and Bo Chen. Mobiledets: Searching for object detection architectures for mobile accelerators. In *Proceedings of the IEEE/CVF conference on computer vision and pattern recognition (CVPR)*, pages 3825–3834, 2021.
- [38] Yuanchao Xu, Mehmet Esat Belviranli, Xipeng Shen, and Jeffrey Vetter. Pccs: Processor-centric contention-aware slowdown model for heterogeneous system-on-chips. In *MICRO-54: 54th Annual IEEE/ACM International Symposium on Microarchitecture*, pages 1282–1295, 2021.
- [39] Tianwei Zhang, Yinqian Zhang, and Ruby B Lee. Dos attacks on your memory in cloud. In *Proceedings of the 2017 ACM on Asia Conference on Computer and Communications Security (CCS)*, pages 253–265, 2017.
- [40] Wu Zhenyu, Xu Zhang, and H Wang. Whispers in the hyper-space: high-speed covert channel attacks in the cloud. In *USENIX Security symposium*, pages 159–173, 2012.